ELSEVIER

Bone 39 (2006) 854–862

BONE

www.elsevier.com/locate/bone

Monitoring individual morphological changes over time in ovariectomized rats by in vivo micro-computed tomography

Steven K. Boyd [a,*], Peter Davison [a], Ralph Müller [b], Jürg A. Gasser [c]

[a] *Department of Mechanical and Manufacturing Engineering, University of Calgary, 2500 University Drive, N.W., Calgary, Alberta, Canada T2N 1N4*
[b] *Institute for Biomedical Engineering, University and ETH Zürich, Zürich, Switzerland*
[c] *Novartis Institutes for Biomedical Research, Basel, Switzerland*

Received 12 February 2006; revised 30 March 2006; accepted 7 April 2006
Available online 6 June 2006

Abstract

The ovariectomized (OVX) rat is a well established model for osteoporosis research. The recent development of in vivo micro-computed tomography (micro-CT) provides new possibilities to monitor individual bone changes over time. The purpose of this study was to establish the normal time course of bone loss in the OVX rat model, and to determine the ability to detect morphological changes in vivo compared to cross-sectional study designs where animals are sacrificed at each time point. Eight-month-old female Wistar rats were randomly assigned to one of two groups: OVX ($N = 10$) or sham-operated ($N = 10$). In vivo micro-CT scanning of the right proximal tibial metaphyses occurred at 1-month intervals for 6 months. Morphological analyses were performed at each time step for every animal, and a two-way ANOVA with repeated measures was used to analyze the data. A second statistical analysis was performed without repeated measures for analysis as a cross-sectional study design. The repeated measures analysis was more sensitive to early changes than the cross-sectional study analysis. Changes were detected by longitudinal analysis in the sham-operated and OVX animals over time ($P < 0.001$) with the exception of trabecular separation in the sham animals. The OVX animals had decreases of bone volume ratio of 33% after 1 month, and 72% after 3 months relative to baseline measurements. Significant changes in bone volume ratio, trabecular number and separation were detected early using a longitudinal analysis, thus in vivo assessment is well poised to enable the study of early treatment protocols on the effects of bone architecture. The in vivo analysis found significant changes in the sham animals which were not detected by the cross-sectional analysis, and the changes to the OVX animal morphology was detected sooner. A substantial variation of baseline morphometry within the homogenous group of rats and response to OVX was observed, thus emphasizing the advantage of performing in vivo analysis where each animal acts as its own control. These data provide new insight into individual bone changes following OVX, and can be used as baseline information upon which future in vivo studies can be designed.

Keywords: Osteoporosis; Osteopenia; Bone histomorphometry; Rat; Tibial metaphyses; Micro-computed tomography; Histomorphometry

Introduction

Osteoporosis is a disease characterized by low bone mass and an increased risk of fragility fractures [1]. The ovariectomized (OVX) rat is an important small animal model for studying the effects of estrogen loss on bone quality [2]. Although a consensus on the precise definition of bone quality is still emerging [3], three-dimensional (3D) micro-architecture is a significant component [4]. Measurement of 3D architecture provides unique insight into the underlying bone mineral density changes that are typically observed by planer densitometric methods such as dual X-ray absorptiometry (DXA). It has been shown in the rat model that there is a rapid decline of trabecular bone volume following ovariectomy [5,6], and that 3D cancellous connectivity loss may be a marker of irreversible architectural damage [7–9].

The vast majority of studies investigating the time course of architectural changes in small animal models have utilized a cross-sectional study design where cohorts of animals are killed at strategic time points after an intervention such as ovariectomy or tail suspension [5,6,10–12]. Cross-sectional designs have been necessary, because, until recently, micro-computed tomography (micro-CT), which provides a non-destructive method to assess 3D bone micro-architecture, could only be performed in vitro.

* Corresponding author. Fax: +1 403 282 8406.
E-mail address: skboyd@ucalgary.ca (S.K. Boyd).

8756-3282/$ - see front matter © 2006 Elsevier Inc. All rights reserved.
doi:10.1016/j.bone.2006.04.017

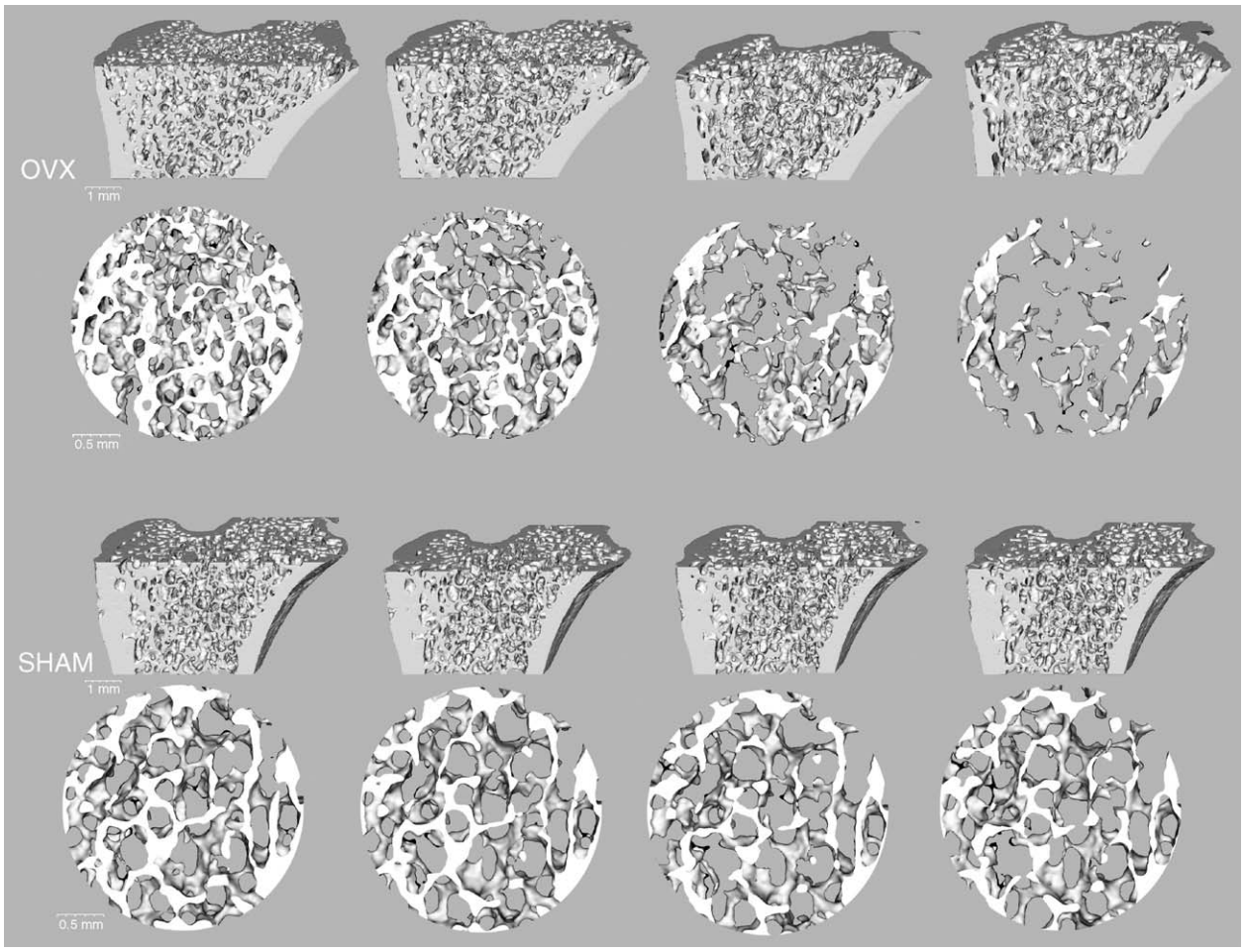

Fig. 1. Three-dimensional images of the tibial metaphysis of an OVX and sham-operated animal (median from each group) at the time of operation and follow-up measurements 1, 2 and 3 months later. The image data are transected to illustrate the internal trabecular structure, and all images were aligned using 3D image registration [33]. Details from each time point (0.3 mm slice) are illustrated in circular cutouts.

The advent of in vivo measurements was first introduced using synchrotron radiation microtomography to assess 3D trabecular bone architecture in laboratory animals [8,13,14], and very recently compact in vivo micro-CT systems have been developed which are more accessible to laboratories for performing longitudinal studies [15,16]. The advantage of a longitudinal study design is that each animal acts as its own control. Thus, normal variations within a cohort are less prone to mask subtle morphological effects, and smaller numbers of animals are needed. The effects of interventions can be assessed on an individual basis, and this may provide valuable information for the increasing volume of research emphasizing the relation between genotype and phenotype [10,17–21].

In this study, we applied the techniques of in vivo micro-CT to establish the time course of architectural changes in ovariectomized rats at the tibial metaphyses on an individual basis. These data establish a useful basis on which future in vivo study designs can be based. Three-dimensional morphological analysis tools were used to quantify the structural changes in a longitudinal (repeated measures) study design. To assess the merits of performing in vivo over in vitro measurement approaches for detecting morphological changes, these same data were reanalyzed by the statistical methods used for a cross-sectional study design.

Methods

Animals

Twenty-eight-month-old female Wistar rats (BRL, Füllinsdorf, Switzerland) weighing on average 260 g were included in the study. They were randomly assigned to one of two groups; ovariectomy was performed on one group (OVX; $N = 10$) by the dorsal approach, and sham operations were performed on the second group (SHAM; $N = 10$). Animals were housed at 25°C with a 12:12-hour light–dark cycle. Animals were housed in groups of five and provided with a standard laboratory diet containing 0.8% phosphorus and 1.1% calcium (NAFAG 890, Basel, Switzerland) and water ad libitum. Studies described herein were performed according to the animal permit BS575 and were approved by the Kantonales Veterinäramt, Basel, Switzerland. All animal experimentations were conducted in accordance with accepted standards of humane animal care.

Micro-CT imaging

Micro-CT scanning was performed in vivo (vivaCT 40, Scanco Medical, Bassersdorf, Switzerland) on each animal at 1-month intervals for 6 months beginning at 8 months (8, 9, 10, 11, 12, 13. 14 months). Rats were anesthetized (isoflurane) and maintained on anesthetic gases for the duration of each measurement (approximately 10 min per rat). The right hind limb was positioned in a custom jig such that the proximal tibial metaphysis of that limb could be scanned without irradiating the contralateral limb. The scans were performed distally from the growth plate (55 kV, 145 μA, 300 ms integration time, 2000 projections on 360°, 2048 CCD detector array, cone-beam reconstruction). Out of

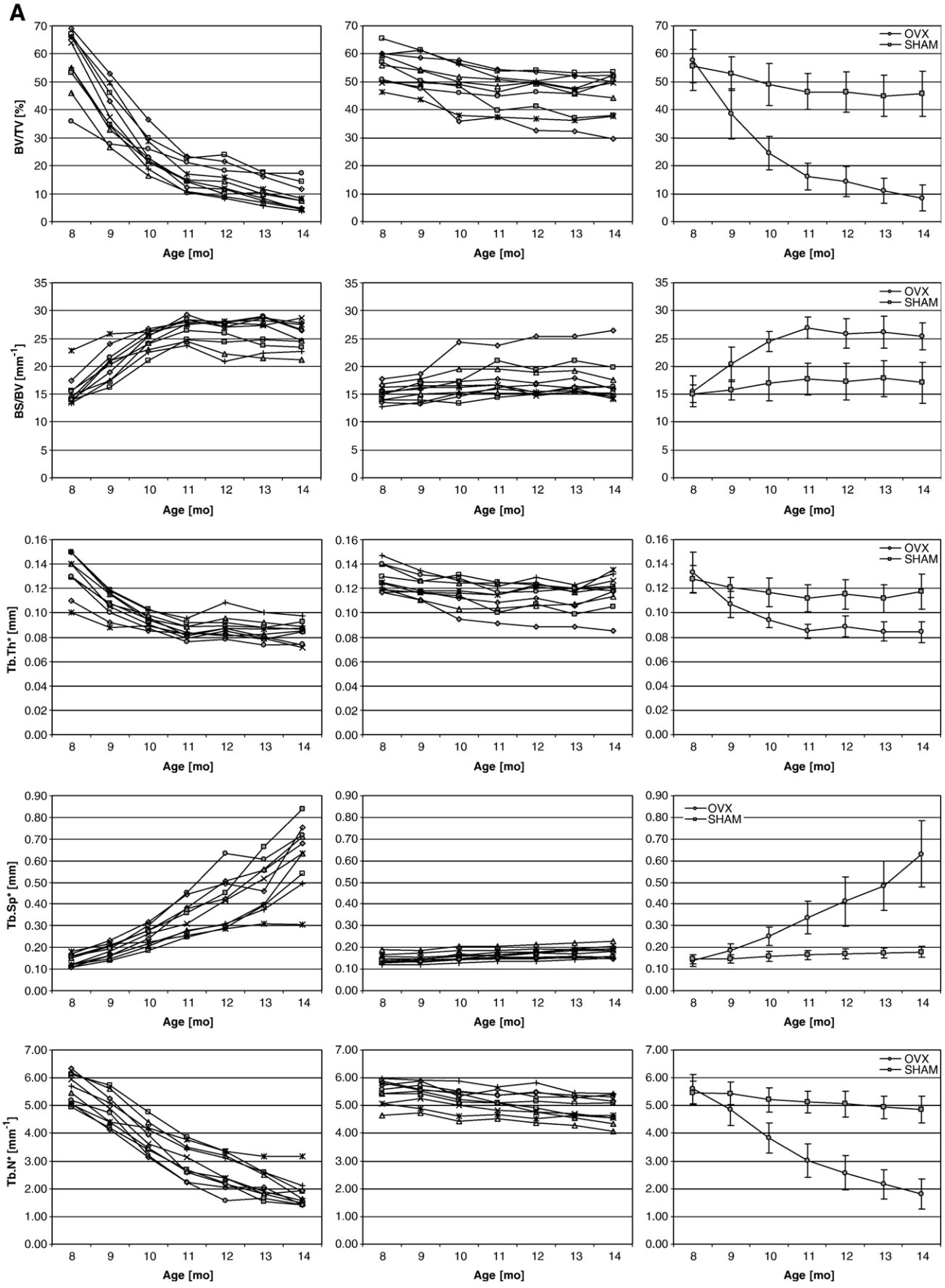
A
BV/TV [%]
BS/BV [mm^{-1}]
Tb.Th* [mm]
Tb.Sp* [mm]
Tb.N* [mm^{-1}]
Age [mo]
OVX
SHAM

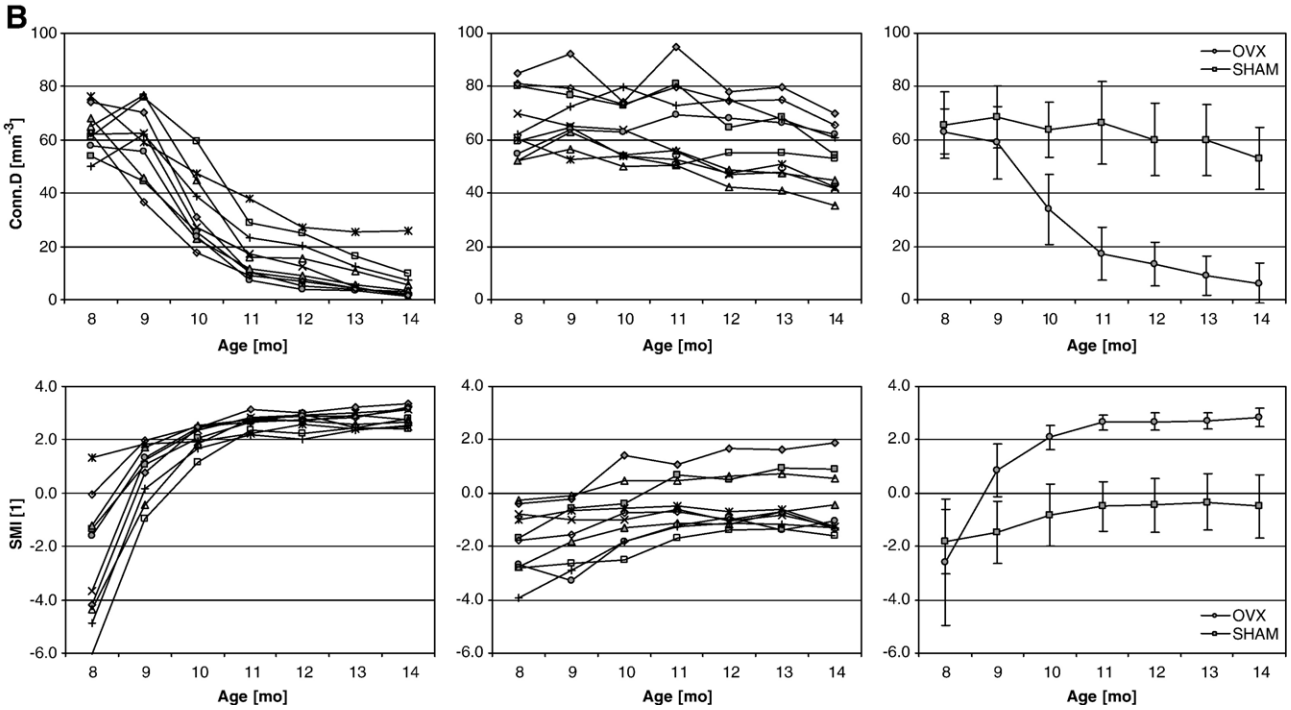

Fig. 2. (A) Individual morphological parameters for each OVX and sham-operated rat (left and middle columns, respectively), and the group means and standard deviations (right column). The OVX and sham operations were performed when the rats were 8 months old. The same line marker is used for each rat for all the OVX plots (similarly for SHAM plots) to aid the reader to identify individual trends. (B) Individual morphological parameters for each OVX and sham-operated rat (left and middle columns), and the group means and standard deviations (right column). The OVX and sham operations were performed when the rats were 8 months old. The same line marker is used for each rat for all the OVX plots (similarly for SHAM plots) to aid the reader to identify individual trends.

this measurement volume, a region located 1.0 mm below the lower end of the growth plate and extending 3.2 mm distally was chosen for evaluation. Nominal isotropic resolution was 15 μm, and the analysis region was represented by 212 micro-tomographic slices. The delivered dose of 0.5 Gy (CTDI) was calculated based on manufacturer specifications. The rats were killed after the final measurement with an overdose of Forene® (isoflurane; Abbott AG, Baar, Switzerland).

Morphological analysis

The trabecular and cortical regions were separated by semi-automatically drawn contours [11,12], and the complete secondary spongiosa of the proximal tibia was evaluated. The resulting gray-scale images were Gaussian filtered ($\sigma = 1.2$, support = 1) and globally thresholded (17.5% of maximum gray value) to form binarized images on which morphological analyses were performed. Three-dimensional analysis techniques were utilized (Image Processing Language, Scanco Medical, Bassersdorf, Switzerland) to assess bone volume ratio (BV/TV), bone surface ratio (BS/BV), trabecular thickness (Tb.Th), trabecular separation (Tb.Sp), trabecular number (Tb.N) [22], connectivity density (Conn.D) [23] and structural model index (SMI) [24].

Each animal was measured at seven time points, therefore in vivo changes of the morphological parameters over the study duration were determined and analyzed as a repeated measures study design. As there are few in vivo micro-CT studies available, it was of interest to contrast the results of the repeated measures analysis with an analysis of the same data treated as a traditional cross-sectional study design (i.e., where cohorts of animals are killed at each time point).

Statistical analysis

Descriptive statistics of all variables were determined including the mean and standard deviation of each group as well as the monthly change and 95% confidence interval. Results were considered to be statistically significant at $P < 0.05$. The results from individual rats as well as group averages were plotted.

A repeated measures two-way ANOVA for all continuous dependent variables determined if there was (a) a time by group interaction effect and (b) a time effect. When F values corresponding to a time by group interaction effect for a given variable were found to be significant, simple effects testing was performed to determine a time effect within each experimental group. Subsequently, paired t tests relative to baseline variables for each time point determined the earliest detectable change, and paired t tests at each time point relative to the

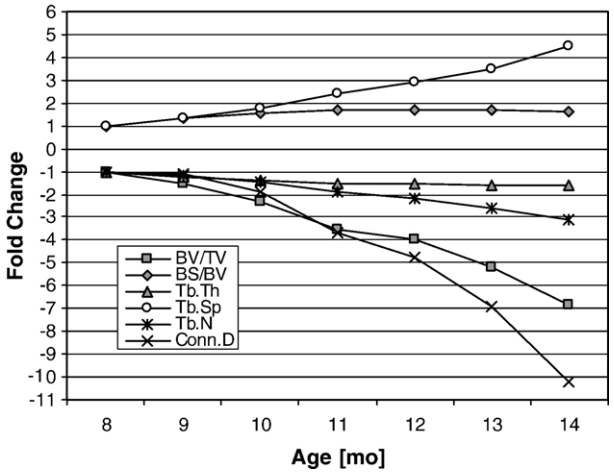

Fig. 3. The change of the morphological parameters from baseline in the OVX rats. The fold change was calculated by dividing the morphological value at each month by its corresponding baseline value. If the number was less than one, then the negative reciprocal is listed. For example, BV/TV at 11 months was 0.28 (i.e., 28%) of the baseline BV/TV, and was reported as a −3.57-fold change.

Table 1
Outcomes by treatment group

		Interaction	Time effect	Age [months]						
				8	9	10	11	12	13	14
BV/TV [%]	SHAM	60.0 (6108) [<0.001†] {<0.001†}	10.2 (6108) [<0.001†] {0.004†}	55.5 ± 6.0	52.9 ± 6.1 −2.6 (−0.9, −4.4) [0.008†] {0.994}	49.0 ± 7.4 −6.6 (−3.8, −9.4) [<0.001†, 0.006†] {0.618, 0.949}	46.5 ± 6.4 −9.1 (−6.2, −11.9) [<0.001†, 0.020†] {0.225, 0.995}	46.4 ± 7.2 −9.2 (−5.5, −12.9) [<0.001†, 0.873] {0.211, 1.000}	45.0 ± 7.3 −10.6 (−6.6, −14.5) [<0.001†, 0.037†] {0.091, 1.000}	45.8 ± 8.1 −9.8 (−4.6, −14.9) [0.002†, 0.335] {0.153, 1.000}
	OVX		198.4 (6108) [<0.001†] {<0.001†}	57.7 ± 10.7	38.6 ± 9.0 −19.1 (−15.6, −22.7) [<0.001†] {<0.001†}	24.5 ± 5.9 −33.2 (−26.5, −39.9) [<0.001†, <0.001†] {<0.001†, 0.004†}	16.2 ± 4.7 −41.6 (−33.8, −49.4) [<0.001†, <0.001†] {<0.001†, 0.291}	14.5 ± 5.3 −43.3 (−35.8, −50.7) [<0.001†, 0.008†] {<0.001†, 0.999}	11.2 ± 4.5 −46.6 (−38.3, −54.8) [<0.001†, 0.001†] {<0.001†, 0.997}	8.4 ± 4.6 −49.3 (−40.4, −58.3) [<0.001†, <0.001†] {<0.001†, 0.991}
BS/BV [mm^{-1}]	SHAM	23.4 (6108) [<0.001†] {<0.001†}	5.0 (6108) [<0.001†] {0.219}	15.1 ± 1.6	15.8 ± 1.8 0.7 (1.2, 0.2) [0.008†] {0.990}	17.0 ± 3.1 1.9 (3.3, 0.5) [0.014†, 0.069] {0.906, 0.992}	17.7 ± 2.9 2.6 (4.1, 1.2) [0.003†, 0.084] {0.660, 0.999}	17.3 ± 03.3 2.2 (4.0, 0.4) [0.021†, 0.273] {0.810, 1.000}	17.8 ± 3.2 2.8 (4.5, 1.0) [0.006†, 0.031†] {0.606, 1.000}	17.1 ± 3.7 2.0 (4.2, 0.2) [0.074, 0.037†] {0.885, 0.999}
	OVX		80.79 (6108) [<0.001†] {<0.001†}	15.5 ± 2.8	20.4 ± 3.0 4.8 (6.1, 3.5) [<0.001†] {<0.011†}	24.5 ± 1.8 8.9 (10.7, 7.2) [<0.001†, <0.001†] {<0.001†, 0.056}	26.9 ± 1.9 11.4 (13.5, 9.2) [<0.001†, <0.001†] {<0.001†, 0.608}	25.9 ± 2.6 10.4 (12.3, 8.4) [<0.001†, 0.025†] {<0.001†, 0.992}	26.2 ± 2.8 10.7 (12.9, 8.4) [<0.001†, 0.403] {<0.001†, 1.000}	25.3 ± 2.4 9.8 (12.0, 7.6) [<0.001†, 0.071] {<0.001†, 0.997}
Tb.Th [mm]	SHAM	20.1 (6108) [<0.001†] {<0.001†}	7.5 (6108) [<0.001†] {0.018†}	0.128 ± 0.011	0.121±0.008 −0.007 (−0.004, −0.010) [0.001†] {0.914}	0.117 ± 0.011 −0.011 (−0.006, −0.017) [0.001†, 0.056] {0.587, 0.997}	0.112 ± 0.011 −0.016 (−0.010, −0.022) [<0.001†, 0.018†] {0.172, 0.991}	0.115 ± 0.012 −0.013 (−0.006, −0.020) [0.003†, 0.048†] {0.428, 0.999}	0.112±0.011 −0.016 (−0.009, −0.023) [<0.001†, 0.010†] {0.149, 0.998}	0.117 ± 0.014 −0.011 (−0.001, −0.020) [0.035†, 0.016†] {0.650, 0.976}
	OVX		78.5 (6108) [<0.001†] {<0.001†}	0.133 ± 0.017	0.107±0.011 −0.026 (−0.021, −0.031) [<0.001†] {<0.001†}	0.094 ± 0.006 −0.039 (−0.002, −0.021) [<0.001†, <0.001†] {<0.001†, 0.219}	0.085 ± 0.006 −0.048 (−0.004, −0.029) [<0.001†, <0.001†] {<0.001†, 0.676}	0.089 ± 0.009 −0.044 (−0.005, −0.036) [<0.001†, 0.028†] {<0.001†, 0.991}	0.085±0.008 −0.048 (−0.005, −0.032) [<0.001†, 0.002†] {<0.001†, 0.987}	0.084 ± 0.009 −0.049 (−0.005, −0.036) [<0.001†, 0.777] {<0.001†, 1.000}
Tb.Sp [mm]	SHAM	59.4 (6108) [<0.001†] {<0.001†}	0.8 (6108) [0.605] {0.893}	0.146 ± 0.021	0.147±0.020 0.001 (0.006, −0.005) [0.797] {1.000}	0.159 ± 0.023 0.013 (0.018, 0.008) [<0.001†, 0.001†] {0.943, 0.954}	0.165 ± 0.020 0.018 (0.024, 0.013) [<0.001†, 0.086] {0.761, 1.000}	0.169 ± 0.023 0.023 (0.029, 0.016) [<0.001†, 0.066] {0.546, 1.000}	0.175±0.023 0.029 (0.038, 0.020) [<0.001†, 0.007†] {0.248, 0.999}	0.180 ± 0.026 0.033 (0.044, 0.022) [<0.001†, 0.027†] {0.109, 1.000}
	OVX		138.0 (6108) [<0.001†] {<0.001†}	0.140 ± 0.027	0.184±0.031 0.044 (0.054, 0.035) [<0.001†] {0.977}	0.251 ± 0.043 0.111 (0.135, 0.087) [<0.001†, <0.001†] {0.301, 0.846}	0.338 ± 0.075 0.198 (0.247, 0.148) [<0.001†, <0.001†] {0.002†, 0.616}	0.412 ± 0.115 0.272 (0.350, 0.193) [<0.001†, 0.001†] {<0.001†, 0.772}	0.485±0.115 0.345 (0.427, 0.262) [<0.001†, 0.012†] {<0.001†, 0.780}	0.631 ± 0.151 0.491 (0.600, 0.382) [<0.001†, <0.001†] {<0.001†, 0.061}
Tb.N [mm^{-1}]	SHAM	93.2 (6108) [<0.001†] {<0.001†}	7.3 (6108) [<0.001†] {0.0490†}	5.461 ± 0.426	5.446±0.395 −0.016 (0.116, −0.148) [0.793] {1.000}	5.210 ± 0.432 −0.251 (−0.138, −0.364) [0.001†, 0.001†] {0.942, 0.957}	5.132 ± 0.382 −0.330 (−0.195, −0.464) [<0.001†, 0.145] {0.812, 1.000}	5.063 ± 0.468 −0.398 (−0.211, −0.585) [0.001†, 0.227] {0.637, 1.000}	4.933±0.415 −0.528 (−0.304, −0.752) [<0.001†, 0.020†] {0.287, 0.998}	4.856 ± 0.476 −0.605 (−0.363, −0.847) [<0.001†, 0.041†] {0.146, 1.000}

	OVX		265.5 (6108) [<0.001†] {<0.001†}	5.597 ± 0.526	4.848±0.569 −0.749 (−0.560, −0.939) [<0.001†] {0.204}	3.826 ± 0.548 −1.771 (−1.439, −2.102) [<0.001†, <0.001†] {<0.001†, 0.020†}	3.010 ± 0.606 −2.587 (−2.131, −3.042) [<0.001†, <0.001†] {<0.001†, 0.127}	2.578 ± 0.630 −3.020 (−2.540, −3.499) [<0.001†, <0.001†] {<0.001†, 0.814}	2.164±0.527 −3.433 (−2.930, −3.935) [<0.001†, 0.002†] {<0.001†, 0.845}	1.805 ± 0.540 −3.792 (−3.244, −4.340) [<0.001†, 0.006†] {<0.001†, 0.914}
Conn.D [mm^{-3}]	SHAM	54.3 (6108) [<0.001†] {<0.001†}	7.5 (6108) [<0.001†] {0.0560}	65.65 ± 12.41	68.64±11.75 2.99 (7.85, −1.87) [0.197] {1.000}	63.82 ± 10.51 −1.83 (4.45, −8.11) [0.527, 0.059] {1.000, 0.994}	66.27 ± 15.54 0.62 (7.29, −6.04) [0.837, 0.388] {1.000, 1.000}	60.04 ± 13.52 −5.60 (2.54, −13.74) [0.154, 0.020†] {0.986, 0.976}	59.95±13.21 −5.69 (1.01, −12.39) [0.087, 0.928] {0.985, 1.000}	52.96 ± 11.62 −12.68 (−4.86, −20.51) [0.005†, <0.001†] {0.554, 0.957}
	OVX		151.3 (6108) [<0.001†] {<0.001†}	63.10 ± 8.31	58.84±13.50 −4.27 (6.14, −14.67) [0.378] {0.998}	33.85 ± 13.30 −29.25 (−18.75, −39.75) [<0.001†, <0.001†] {<0.001†, <0.001†}	17.25 ± 9.91 −45.86 (−37.80, −53.91) [<0.001†, <0.001†] {<0.001†, 0.046}	13.33 ± 8.31 −49.77 (−42.19, −57.35) [<0.001†, 0.001†] {<0.001†, 0.993}	9.12 ± 7.23 −53.98 (−47.46, −60.50) [<0.001†, 0.001†] {<0.001†, 0.989}	6.16 ± 7.48 −56.94 (−50.85, −63.03) [<0.001†, 0.001†] {<0.001†, 0.998}
SMI [1]	SHAM	20.9 (6108) [<0.001†] {<0.001†}	6.4 (6108) [<0.001†] {0.010†}	−1.816 ± 1.208	−1.470±1.148 0.346 (0.737, −0.046) [0.077] {0.998}	−0.830 ± 1.155 0.986 (1.493, 0.479) [0.002†, 0.007†] {0.681, 0.945}	−0.491 ± 0.931 1.325 (1.881, 0.769) [<0.001†, 0.033†] {0.321, 0.998}	−0.453±1.022 1.363 (2.029, 0.696) [0.001†, 0.721] {0.287, 1.000}	−0.348±1.058 1.468 (2.116, 0.820) [0.001†, 0.256] {0.204, 1.000}	−0.496 ± 1.195 1.320 (2.150, 0.490) [0.006†, 0.231] {0.325, 1.000}
	OVX		76.5 (6108) [<0.001†] {<0.001†}	−2.605 ± 2.365	0.867±0.993 3.473 (4.596, 2.350) [<0.001†] {<0.001†}	2.097 ± 0.447 4.702 (6.246, 3.158) [<0.001†, <0.001†] {<0.001†, 0.303}	2.647 ± 0.291 5.252 (6.967, 3.538) [<0.001†, <0.001†] {<0.001†, 0.959}	2.670 ± 0.322 5.276 (6.892, 3.660) [<0.001†, 0.692] {<0.001†, 1.000}	2.741±0.291 5.319 (7.052, 3.586) [<0.001†, 0.600] {<0.001†, 1.000}	2.854 ± 0.347 5.459 (7.138, 3.781) [<0.001†, 0.027†] {<0.001†, 1.000}
Legend		$F(df)$ [P] {P_x}	$F(df)$ [P] {P_x}	MN ± SD	MN ± SD Δ (CI) [P_{base}] {$P_{x,base}$}	MN ± SD Δ (CI) [P_{base}, P_{time}] {$P_{x,base}$, $P_{x,time}$}	MN ± SD Δ (CI) [P_{base}, P_{time}] {$P_{x,base}$, $P_{x,time}$}	MN ± SD Δ (CI) [P_{base}, P_{time}] {$P_{x,base}$, $P_{x,time}$}	MN ± SD Δ (CI) [P_{base}, P_{time}] {$P_{x,base}$, $P_{x,time}$}	MN ± SD Δ (CI) [P_{base}, P_{time}] {$P_{x,base}$, $P_{x,time}$}

Interaction and time effects are reported ($F(df)$), and P values are reported for the repeated measures analysis (square brackets [ ]) and cross-sectional study design (curly brackets {}). Measurements for each month include group averages (mean ± SD), and changes with respect to baseline values and a 95% confidence interval of the magnitude of change. Two P values are reported for each repeated measures and cross-sectional analyses. The first P value represents change with respect to baseline, and the second P value represents change with respect to previous measure. The P values less than 0.05 are indicated (†).

previous time point determined if there were significant changes from month to month.

Contrasting with the repeated measures analysis above, the same data were re-examined as a cross-sectional study design. A two-way ANOVA determined (a) time by group interaction effect and (b) time effect. When appropriate, based on F values, simple effects testing determined a time effect within each experimental group. Finally, Scheffé post hoc tests and linear contrasts were performed relative to each baseline variable to determine when significant changes were first detected, and relative to the previous month change to determine the change from month to month.

Results

All 20 rats completed the study and in vivo micro-CT measurements were obtained at each time point providing an assessment of the morphological changes within each individual rat (Fig. 1). The individual morphological change over the study duration as well as group averages and standard deviations are presented (Fig. 2), in addition to the fold-change from baseline of the morphological parameters for the OVX group (Fig. 3). A detailed description of the group averages, and change relative to baseline values with 95% confidence intervals are provided, and the statistical significance of those changes as determined by both the repeated-measures and cross-sectional analysis study designs are included (Table 1). There was a substantial change in the morphological parameters in the OVX animals, and although the largest changes presented in the first three months, the trends continued for the duration of the study. The sham animals changed considerably less than the OVX group, yet the change continued for the duration of the study.

There was significant interaction between time and group for all of the morphological parameters. Subsequently, simple effects testing verified that there was an effect of time within both sham and OVX groups for all morphological parameters with the only exception being no detected change in Tb.Sp of the sham-operated rats. In the sham-operated rats, BV/TV, BS/BV and Tb.Th change was detected 1 month from the start of the study ($P = 0.008$, $P = 0.008$, $P = 0.001$, respectively), and the Tb.N and SMI change was detected at 2 months ($P = 0.001$, $P = 0.002$, respectively). The Conn.D change relative to baseline became significant at the seventh measurement ($P = 0.005$) for the shams. In the OVX groups, all the morphological parameters changed significantly with respect to time, and significant changes were detected 1 month from the start of the study ($P < 0.001$) except for Conn.D where the first detected change occurred after 2 months ($P < 0.001$). A continuous change from month to month for BV/TV, Tb.Sp, Tb.N and Conn.D in the OVX animals was detected for the duration of the study ($P = 0.012$ or less for all changes), whereas the Tb.Th may have reached an asymptote at 14 months ($P = 0.777$), and the SMI did not change from 11 to 13 months ($P = 0.692$, $P = 0.600$). Increasing BS/BV seemed to level off at around 4 months.

In contrast to the results based on a repeated measures analysis of the in vivo data, analysis of the data using the cross-sectional study design revealed less sensitivity to the effects of the sham OVX with respect to time. Interaction between groups and time, as well as simple effects testing of morphological changes with time showed significant changes ($P = 0.018$ and lower) as was found by the repeated measures analysis; the only exception was no effect of time found in the Conn.D sham animals. Neither the change of the sham animals relative to baseline nor the change of the sham animals from month to month was detected. Morphological changes of the OVX group for BV/TV, Tb.Th, SMI and Conn.D were detected at the same time point as per the repeated measures analysis; however, the first changes to Tb.N were not detected until 10 months ($P < 0.001$) and changes to Tb.Sp were not detected until 11 months ($P < 0.002$) whereas change in both of these parameters was determined to have occurred 1 and 2 months earlier, respectively, as per the repeated measures analysis. The change in morphological parameters in the OVX animals from month to month for the majority of measures was not significant which contrasts the repeated measures results.

Discussion

The time course of bone architectural changes in a rat model of osteoporosis was determined in vivo by micro-CT measurements of the proximal tibia for 6 months. The rats receiving the OVX operation had a large decrease in bone volume ratio and associated morphological parameters as expected, and that decrease was greatest in the first 3 months. The sham-operated rats also changed, although the changes were much smaller than in the OVX group. The novelty of these data is that this is the first time in vivo longitudinal changes to bone architecture were monitored in two substantially sized groups of rats (OVX and sham), thus enabling statistically clear identification of stages of bone loss during a six month period.

Estrogen deficiency due to the OVX operation had a potent effect on bone architectural changes in the tibial metaphysis of the rat, and significant changes were detected at the first follow-up measurement for all parameters except connectivity density which changed only in the second month. The decrease in bone volume ratio after 2 months was 57% compared to the baseline values, and this is consistent with the findings of others performing in vivo measurements where approximately 50% bone volume ratio loss was reported after a slightly shorter time period (50 days) [9,14]. In contrast, other studies have reported larger decreases of bone loss where, for example, a 40% decrease was found after only 12 days [11], and a 60% decrease by 1 month [16] compared to only 33% loss after 1 month in the present study. The reason for this difference is not clear; however, both of those studies used Sprague–Dawley rats instead of Wistar rats, and it is possible that the different breeds respond differently to OVX. Another notable difference from past reports is that a reversing trend toward increased trabecular thickness at approximately 14 weeks following OVX [11,16] was not observed in this in vivo cohort. It should be pointed out that neither of those studies found the reversing trend to be statistically significant which may be related to a small cohort ($N = 1$; [16]) or a insufficient statistical power of a cross-sectional design [11]. Nevertheless, in this study, significantly decreasing trabecular thickness was detected for every time step except for the final measurement 24 weeks after OVX where a

possible asymptote may have been reached. Additionally, early changes to connectivity density previously reported [11] were not detected immediately in the current study, although it was significantly changed by 2 months. This may be due to differences in animal ages or assessment sites. Finally, consistent with past studies, it was clear that the bone became more rod-like after OVX as measured by the structural model index [11], and this change was detected at the first follow-up measurement. The changing structure emphasizes the importance of using direct measurement methods of the 3D data for assessment of parameters such as trabecular thickness, separation and number [22].

The sham-operated rats also had changes to their bone architecture during the 6-month study period, although the changes were an order of magnitude less than changes in the OVX animals. Significant decreases in bone volume ratio and trabecular thickness were detected after 1 month, while trabecular number and the structural model index were altered after 2 months. Connectivity density decreases were significant only at the end of the study, and there was no detected change in trabecular separation in the sham animals. It is possible that the changes in the sham rats are due to normal aging as decreases in bone mineral density have been reported by others [25], particularly starting near the age of 9 months [26,27]. Also, the lack of connectivity density change is consistent with previous reports [28]. Of course, an important factor that could contribute to the changes in the sham animals is the effect of radiation or anesthesia during the repeated in vivo micro-CT scans. The 0.5 Gy dose (CTDI) received by the animals was small, but not negligible, and may influence the biological pathways affecting bone remodeling [29]. The effect of radiation on bone is not well understood, but recent work in our laboratory has used the non-irradiated contralateral limb as a control in three inbred strains of mice measured weekly for 4 weeks, and it was found that the bone volume ratio of the irradiated limbs was decreased by at most 3% [30]. The radiation effect likely differs between rats and mice; however, the results of the current study clearly demonstrate that if in fact there is an effect of radiation, it is small compared to the changes due to OVX. Future studies using in vivo micro-CT would be well advised to measure the non-irradiated contralateral limb to act as an internal control for the effect of radiation at the end of the study.

The changes to the OVX animals predominantly occurred in the first 3 months following OVX; however, they continued for the duration of the entire study. The decrease in trabecular bone volume ratio in months 1 to 3 were −19.1, −33.2 and −41.6%, respectively, resulting in a relative decrease of 72% from baseline by the end of that period. This early trend is also apparent in parameters such as the structure model index, where the conversion from a plate-like to rod-like structure predominantly occurred in the first 3 months. Thus, in those early months, it would appear that trabecular thinning leads to removal of the thinner structures, followed by progressively thicker structures until indices such as connectivity density are affected. The lack of significant alterations to connectivity density until the second month indicates that there may be an important window of opportunity early after OVX. Treatment by anti-catabolic drugs (i.e., bisphosphonates) may be able to preserve the existing architecture in this early window. Similarly, anabolic drugs (i.e., parathyroid hormone treatment) may result in bone apposition; however, the restoration of the original structure is problematic [31,32], thus for the same level of bone strength, a relatively increased bone mass would be required. Therefore, intervening in the early stages before significant architectural changes have occurred, although not an absolute necessity, would seem to be advantageous from the point of view of maintaining an optimized structure in terms of the ratio of bone mass to strength. In future in vivo micro-CT studies, increasing the frequency of measurements in the first three months may provide improved time-lapse insight into the early architectural changes.

Performing studies using in vivo micro-CT has the advantage of reducing the number of animals used in the study while at the same time increasing the sensitivity of the experiment to detect subtle changes. The same study based on in vitro micro-CT measurements would require a sevenfold increase in the number of animals, and have less sensitivity to detect morphological change. Since each animal acts as its own control, the variability that is normally present within a cohort of animals is accommodated and changes are more readily detected by paired comparisons. As demonstrated, the analysis of the in vivo data using a cross-sectional design approach was unable to detect any change in the sham animals relative to baseline values. Furthermore, in the OVX group, changes in trabecular number and trabecular separation were detected 1 and 2 months later, respectively, and changes from month to month were not detected for any of the morphological parameters. Even in a homogenous group of animals, there is substantial variation within a cohort and in vivo micro-CT analysis can help overcome this barrier through repeated measures. Further improvements to measurement sensitivity could entail the use of 3D image registration to ensure identical sample regions within a subject over time [16,33]. Finally, despite the similar genetic backgrounds, the response to OVX appears to differ among animals (i.e., BV/TV)—an observation only possible through in vivo measurements.

In summary, the time course of architectural changes in a rat model of osteoporosis has been presented which provides important baseline data such that future in vivo studies can be designed to target specific time points of expected changes for interventions of either a mechanical or pharmaceutical nature, and the ability to sensitively evaluate the structural changes by in vivo analysis in both OVX and sham animals was demonstrated.

Acknowledgments

The authors wish to acknowledge the support of Dr. Tak Fung for his assistance with the statistical analysis.

References

[1] Kanis JA. Osteoporosis. Oxford: Blackwell Science Ltd.; 1994.
[2] Mosekilde L. Assessing bone quality-animal models in preclinical osteoporosis research. Bone 1995;17:343S–52S.
[3] Bone quality: what is it and can we measure it? NIAMS-ASBMR Scientific Meeting. Maryland: Bethesda; 2005.

[4] Dempster DW. The contribution of trabecular architecture to cancellous bone quality. J Bone Miner Res 2000;15:20–3.
[5] Wronski TJ, Dann LM, Horner SL. Time course of vertebral osteopenia in ovariectomized rats. Bone 1989;10:295–301.
[6] Wronski TJ, Dann LM, Scott KS, Cintron M. Long-term effects of ovariectomy and aging on the rat skeleton. Calcif Tissue Int 1989;45:360–6.
[7] Kinney JH, Haupt DL, Balooch M, Ladd AJ, Ryaby JT, Lane NE. Three-dimensional morphometry of the L6 vertebra in the ovariectomized rat model of osteoporosis: biomechanical implications. J Bone Miner Res 2000;15:1981–91.
[8] Lane NE, Thompson JM, Haupt D, Kimmel DB, Modin G, Kinney JH. Acute changes in trabecular bone connectivity and osteoclast activity in the ovariectomized rat in vivo. J Bone Miner Res 1998;13:229–36.
[9] Lane NE, Haupt D, Kimmel DB, Modin G, Kinney JH. Early estrogen replacement therapy reverses the rapid loss of trabecular bone volume and prevents further deterioration of connectivity in the rat. J Bone Miner Res 1999;14:206–14.
[10] Bouxsein ML, Myers KS, Shultz KL, Donahue LR, Rosen CJ, Beamer WG. Ovariectomy-induced bone loss varies among inbred strains of mice. J Bone Miner Res 2005;20:1085–92.
[11] Laib A, Kumer JL, Majumdar S, Lane NE. The temporal changes of trabecular architecture in ovariectomized rats assessed by MicroCT. Osteoporos Int 2001;12:936–41.
[12] Laib A, Barou O, Vico L, Lafage-Proust MH, Alexandre C, Rüegsegger P. 3D micro-computed tomography of trabecular and cortical bone architecture with application to a rat model of immobilisation osteoporosis. Med Biol Eng Comput 2000;38:326–32.
[13] Kinney JH, Lane NE, Haupt DL. In vivo, three-dimensional microscopy of trabecular bone. J Bone Miner Res 1995;10:264–70.
[14] Kinney JH, Ryaby JT, Haupt DL, Lane NE. Three-dimensional in vivo morphometry of trabecular bone in the OVX rat model of osteoporosis. Technol Health Care 1998;6:339–50.
[15] David V, Laroche N, Boudignon B, Lafage-Proust MH, Alexandre C, Rüegsegger P, et al. Noninvasive in vivo monitoring of bone architecture alterations in hindlimb-unloaded female rats using novel three-dimensional microcomputed tomography. J Bone Miner Res 2003;18:1622–31.
[16] Waarsing JH, Day JS, van der Linden JC, Ederveen AG, Spanjers C, De Clerck N, et al. Detecting and tracking local changes in the tibiae of individual rats: a novel method to analyse longitudinal in vivo micro-CT data. Bone 2004;34:163–9.
[17] Turner CH, Hsieh YF, Muller R, Bouxsein ML, Baylink DJ, Rosen CJ, et al. Genetic regulation of cortical and trabecular bone strength and microstructure in inbred strains of mice. J Bone Miner Res 2000;15:1126–31.
[18] Beamer WG, Donahue LR, Rosen CJ, Baylink DJ. Genetic variability in adult bone density among inbred strains of mice. Bone 1996;18:397–403.
[19] Beamer WG, Donahue LR, Rosen CJ. Genetics and bone. Using the mouse to understand man. J Musculoskelet Neuronal Interact 2002; 2:225–31.
[20] Judex S, Garman R, Squire M, Donahue LR, Rubin C. Genetically based influences on the site-specific regulation of trabecular and cortical bone morphology. J Bone Miner Res 2004;19:600–6.
[21] Koller DL, Schriefer J, Sun Q, Shultz KL, Donahue LR, Rosen CJ, et al. Genetic effects for femoral biomechanics, structure, and density in C57BL/6J and C3H/HeJ inbred mouse strains. J Bone Miner Res 2003;18:1758–65.
[22] Hildebrand T, Rüegsegger P. A new method for the model-independent assessment of thickness in three-dimensional images. J Microsc 1997;185:67–75.
[23] Odgaard A, Gundersen HJ. Quantification of connectivity in cancellous bone, with special emphasis on 3-D reconstructions. Bone 1993;14:173–82.
[24] Hildebrand T, Rüegsegger P. Quantification of bone microarchitecture with the structure model index. Comput Methods Biomech Biomed Eng 1997;1:15–23.
[25] Tanaka M, Toyooka E, Kohno S, Ozawa H, Ejiri S. Long-term changes in trabecular structure of aged rat alveolar bone after ovariectomy. Oral Surg Oral Med Oral Pathol Oral Radiol Endo 2003;95:495–502.
[26] Banu J, Wang L, Kalu DN. Age-related changes in bone mineral content and density in intact male F344 rats. Bone 2002;30:125–30.
[27] Fukuda S, Iida H. Age-related changes in bone mineral density, cross-sectional area and the strength of long bones in the hind limbs and first lumbar vertebra in female Wistar rats. J Vet Med Sci 2004;66:755–60.
[28] Mawatari T, Miura H, Higaki H, Kurata K, Moro-oka T, Murakami T, et al. Quantitative analysis of three-dimensional complexity and connectivity changes in trabecular microarchitecture in relation to aging, menopause, and inflammation. J Orthop Sci 1999;4:431–8.
[29] Boone JM, Velazquez O, Cherry SR. Small-animal X-ray dose from micro-CT. Mol Imaging 2004;3:149–58.
[30] Klinck RJ, Boyd SK. The effect of radiation on bone architecture for in vivo micro-computed tomography. In: 52nd Annual Meeting of the Orthopaedic Research Society. New Orleans; 2006. p. 1596.
[31] Lane NE, Thompson JM, Strewler GJ, Kinney JH. Intermittent treatment with human parathyroid hormone (hPTH[1–34]) increased trabecular bone volume but not connectivity in osteopenic rats. J Bone Miner Res 1995;10:1470–7.
[32] Lane NE, Kumer J, Yao W, Breunig T, Wronski T, Modin G, et al. Basic fibroblast growth factor forms new trabeculae that physically connect with pre-existing trabeculae, and this new bone is maintained with an anti-resorptive agent and enhanced with an anabolic agent in an osteopenic rat model. Osteoporos Int 2003;14:374–82.
[33] Boyd SK, Moser S, Kuhn M, Klinck RJ, Krauze P, Müller R, Gasser JA. Image registration accuracy for in vivo 3D micro-computed tomography. Ann Biomed Eng 2006. [Submitted for publication].